

# Emitter technology options for industrial PERC solar cells with up to 20.3% conversion efficiency

Thorsten Dullweber<sup>1</sup>, Helge Hannebauer<sup>1</sup>, Christopher Kranz<sup>1</sup>, Rene Hesse<sup>1</sup>, Sabrina Wyczanowski<sup>1</sup>, Vikram Bhosle<sup>2</sup> & Chris Dubé<sup>2</sup>, Katrin Weise<sup>3</sup> & Franck Delahaye<sup>3</sup>, Oliver Doll<sup>4</sup>, Ingo Kohler<sup>4</sup>, Rolf Brendel<sup>1</sup>

<sup>1</sup> Institute for Solar Energy Research Hamelin (ISFH), Emmerthal, Germany

<sup>2</sup> Applied Materials, Varian Semiconductor Equipment, Gloucester, Massachusetts, USA

<sup>3</sup> RENA GmbH, Freiburg, Germany

<sup>4</sup> Merck KGaA, Darmstadt, Germany

## ABSTRACT

Passivated emitter and rear cells (PERC) are considered to be a next generation of industrial solar cells, and several companies have already started pilot production. The much-reduced rear-surface recombination in PERC cells requires improvements to the front side, for example the emitter, in order to further increase the conversion efficiency in the future. This paper presents an evaluation of the emitter technologies of three industrially applicable PERC cell concepts: 1) with an ion-implanted emitter, 2) with a chemically polished rear surface, and 3) with a selective emitter formed by gas phase etch-back (GEB). The results are compared with a reference high-efficiency  $\text{POCl}_3$ -diffused PERC cell. The three industrial PERC concepts utilize lean industrially applicable process flows which reduce the phosphorus concentration at the wafer surface. Accordingly, when compared with the  $\text{POCl}_3$ -diffused emitter, the ion-implanted and GEB emitters obtain significantly lower emitter saturation current densities of 40 to 60 fA/cm<sup>2</sup> for emitter sheet resistances of 90 to 130  $\Omega$ /sq. When applied to large-area PERC cells with screen-printed metal contacts, the ion-implanted and GEB emitter cells demonstrate up to 10 mV higher open-circuit voltages than the  $\text{POCl}_3$ -diffused reference PERC cell, and achieve conversion efficiencies of 20.0 and 20.3%, respectively. The next steps in further increasing the efficiency are outlined.

## Introduction

The passivated emitter and rear cell (PERC) concept was first published in 1989 [1] as a high-efficiency laboratory-type solar cell. PERC solar cells have since been intensively evaluated and optimized by industry and research institutes as a next-generation silicon solar cell concept for mass production. Several companies have already announced the pilot production of PERC solar cells [2–5], and efficiencies of up to 21.0% have been demonstrated for large-area PERC cells with screen-printed contacts [6]. Excellent rear-surface recombination velocities below 150 cm/s have been reported, demonstrating the high-efficiency potential of industrial PERC cells [7,8].

Because of the much-reduced carrier recombination at the rear side of PERC cells, the phosphorus emitter now requires further optimization for conversion efficiencies beyond 21.0% to be achieved in the future. To keep production costs low, however, improvements in emitter technology have to be realized using a very lean process flow and as few extra process steps as possible. In recent years, a lot of effort has already been dedicated

to optimizing the phosphorus emitter, in particular with respect to selective emitters [9–14], which are applicable to PERC cells as well.

“The phosphorus emitter now requires further optimization for conversion efficiencies beyond 21.0% to be achieved in the future.”

Four different PERC process flows which yield almost identical rear sides, but result in four different phosphorus emitters, are investigated and compared in this paper:

1. **Ref. PERC:** ISFH reference PERC process flow employing a homogeneously  $\text{POCl}_3$ -diffused 70  $\Omega$ /sq. emitter and a planar rear side obtained by a protection layer.
2. **I<sup>2</sup>-PERC:** PERC process flow where the emitter is formed by phosphorus ion implantation (I<sup>2</sup>) and subsequent annealing.

3. **Polished PERC:** PERC process flow where the rear side is chemically polished after texturing and  $\text{POCl}_3$ -diffusion. The rear polish and subsequent wet cleaning slightly etch back the emitter.

4. **GEB PERC:** PERC process flow where the very reactive gas phase of a modified polishing process is used to form a selective emitter via gas phase etch-back (GEB).

Whereas the reference PERC process serves as a high-efficiency baseline process, the other three PERC process flows are designed to reduce the front-surface phosphorus concentration and hence potentially reduce the emitter saturation current density, allowing higher conversion efficiencies. At the same time, these three industrial PERC process flows incorporate very lean process sequences with the aim of targeting industrial mass production. The emitter doping profiles and saturation current densities, as well as the *I-V* parameters and quantum efficiencies of the resulting PERC solar cells, are reported in this paper.

## The PERC process flows and emitter technologies investigated

Boron-doped Cz wafers of size 156×156mm<sup>2</sup> with a resistivity of 2–3Ωcm and a starting thickness of 190μm are used for all PERC process flows. The four process flows, shown in Table 1, differ in their emitter formation and rear-surface preparation. Process steps which impact the emitter formation are highlighted in green. All four PERC process flows, however, apply the same initial wafer cleaning, alkaline texturing, SiN<sub>x</sub> front-surface passivation, AlO<sub>x</sub>/SiN<sub>y</sub> rear-surface passivation, laser contact opening (LCO), screen printing of Ag front (print-on-print) and Al rear metal contacts, and firing profile, as indicated by the process steps highlighted in blue in Table 1. The resulting PERC cell structures are shown schematically in Fig. 1. An overview of each of the four different PERC process flows of Table 1 and Fig. 1, with an emphasis on the emitter formation, is given next.

### A) Ref. PERC: reference PERC cells with rear protection layer

The process flow for the reference PERC solar cells is described in detail by Dullweber et al. [7]. Before texturing and POCl<sub>3</sub> diffusion, a dielectric protection layer is deposited on the rear side of the wafer, resulting in a planar and non-diffused rear side. A homogeneously doped emitter with a sheet resistance of about 60Ω/sq. measured after diffusion is applied. Because of the subsequent wet cleaning (PSG and dielectric etch, cleaning before rear passivation), the emitter is etched back slightly, which increases the emitter sheet resistance to a final value of around 70Ω/sq. A 10nm-thick atomic layer deposited (ALD) AlO<sub>x</sub> layer is applied to the rear side. A plasma-enhanced chemical vapour deposition (PECVD) SiN<sub>y</sub> capping layer is then deposited on top of the AlO<sub>x</sub> passivation layer at the rear in order to improve both the optical reflectivity and the surface passivation quality.

The emitter is covered with a PECVD SiN<sub>x</sub> anti-reflective coating. To form local line openings, the dielectric layer stack at the rear is locally ablated by LCO [7,15]. Line contacts were chosen instead of point contacts, since the former facilitate the formation of a deep and uniform local Al-BSF [16]. The Ag front contacts are deposited by a print-on-print (PoP) screen-printing process, resulting in a finger width of around 60μm [17]. The Al rear contact is formed by full-area Al screen printing of a commercially available Al paste designed for local rear contacts. In total, 11 process steps are necessary for this reference PERC process flow, resulting in the PERC solar cell shown schematically in Fig. 1 (left).

### B) I<sup>2</sup>-PERC: PERC solar cells with ion-implanted phosphorus emitter

As an alternative to POCl<sub>3</sub> diffusion, emitter formation by ion implantation is evaluated; see Dullweber et al. [18] for a detailed description of the I<sup>2</sup>-PERC process flow. A single-

A: Ref. PERC	B: I <sup>2</sup> -PERC	C: Polished PERC	D: GEB PERC
Wafer cleaning	Wafer cleaning	Wafer cleaning	Wafer cleaning
Rear protection layer	Rear protection layer		
Texturing	Texturing	Texturing	Texturing
Phosphorus diffusion	Ion implantation	Phosphorus diffusion	Phosphorus diffusion
PSG + dielectric etch	Anneal		Front: etch barrier
	Front: SiN <sub>x</sub>	Rear: Polish	Polish + GEB
Rear: AlO <sub>x</sub> /SiN <sub>y</sub>	Rear: dielectric etch	Rear: AlO <sub>x</sub> /SiN <sub>y</sub>	Rear: AlO <sub>x</sub> /SiN <sub>y</sub>
Front: SiN <sub>x</sub>	Rear: AlO <sub>x</sub> /SiN <sub>y</sub>	Front: SiN <sub>x</sub>	Front: SiN <sub>x</sub>
Rear: laser ablation	Rear: laser ablation	Rear: laser ablation	Rear: laser ablation
Ag screen printing	Ag screen printing	Ag screen printing	Ag screen printing
Al screen printing	Al screen printing	Al screen printing	Al screen printing
Co-firing	Co-firing	Co-firing	Co-firing
11 steps	12 (10) steps	10 steps	11 steps

**Table 1. Process flows of the reference PERC cell (A), as well as the three industrially applicable PERC cell concepts with ion-implanted emitter (B), chemically polished rear surface (C) and selective emitter by gas phase etch-back (GEB) (D). The ‘green’ process steps impact the emitter formation, whereas the ‘blue’ process steps are identical for all four PERC process flows.**

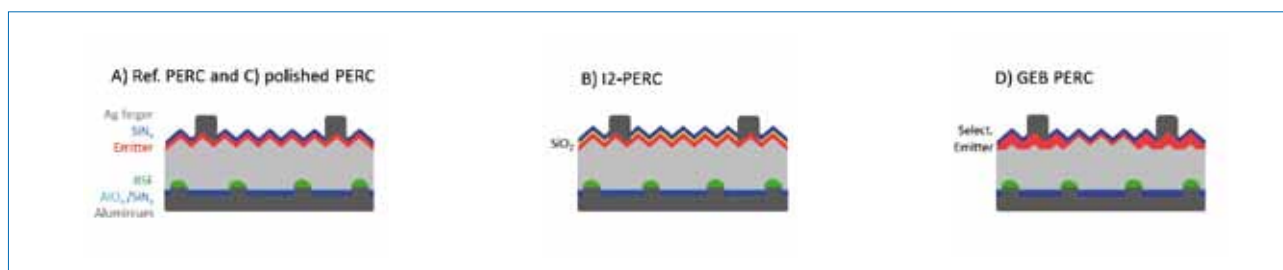


**Figure 1. Schematic cross sections of the four PERC cells resulting from the different process flows in Table 1.**

sided texturing of the front side is obtained by using a rear protection layer, which is later removed in the process flow. The phosphorus emitter is ion implanted using an implanter similar to the Applied Materials Solion tool [13]. Afterwards, the crystal damage caused by the ion implantation is annealed in a high-temperature step, which activates the phosphorus doping, resulting in an emitter sheet resistance of around  $65\Omega/\text{sq}$ . A thin thermal oxide is then grown in the furnace as part of the anneal, providing surface passivation of the emitter. A  $\text{SiN}_x$  anti-reflective coating is deposited on the front side, and the dielectric layer on the wafer rear side is then removed. Next, the  $\text{AlO}_x/\text{SiN}_y$  passivation stack is deposited on the wafer rear side. The LCO and the screen printing of the front and rear contacts is performed as described above for the reference PERC process flow.

The resulting PERC solar cell is shown schematically in Fig. 1 (centre); this cell differs from the reference PERC cell in its emitter doping profile and  $\text{SiO}_2/\text{SiN}_y$  front-surface passivation. A future option for a very lean process flow with industrial manufacturing in mind is to skip the rear protection layer and apply a single-sided alkaline texturing or a chemical rear polish after double-sided texturing as in the polished PERC cell (described in the next section). This would allow the dielectric etch (later in the process flow) to also be skipped, so that only 10 steps in total would be required for the PERC cell processing.

### C) Polished PERC: PERC solar cells with polished rear side

The process flow for the polished PERC cell is described in detail by Kranz et al. [19]. After double-sided alkaline texturing, the emitter is formed by  $\text{POCl}_3$  diffusion, resulting in an emitter sheet resistance of  $45\Omega/\text{sq}$ . after diffusion. The RENA InPilot tool is then used to take off about  $5\mu\text{m}$  of silicon from the rear surface by single-sided wet chemical polishing; this removes the rear-side emitter and smooths the rear surface. After the polishing step, a cleaning sequence is carried out prior to depositing the  $\text{AlO}_x/\text{SiN}_y$  rear passivation layer. The polishing process, and even more so the subsequent wet cleaning, slightly etch back the emitter, which increases the emitter sheet resistance from the initial  $45\Omega/\text{sq}$ . to around  $65\Omega/\text{sq}$ . The passivation of the rear and front surfaces, the LCO and the screen printing of the front and rear contacts are performed as described

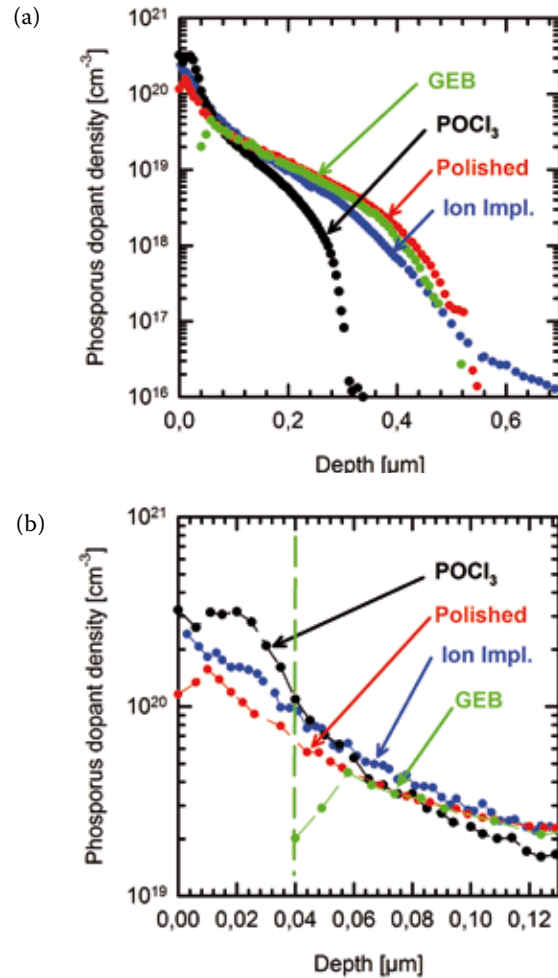


Figure 2. (a) Doping profiles of the ion-implanted phosphorus emitter ( $65\Omega/\text{sq}$ ), the emitter after polishing ( $65\Omega/\text{sq}$ ) and the gas phase etch-back (GEB) emitter ( $90\Omega/\text{sq}$ , shifted by  $40\text{nm}$ ) measured by ECV profiling. The doping profile of the  $\text{POCl}_3$ -diffused emitter ( $70\Omega/\text{sq}$ ) is included as a reference. (b) Close-up of the front surface in Fig. 2(a). The dashed green line denotes the removal of around  $40\text{nm}$  of silicon by the GEB process. The lower concentration of surface phosphorus of the GEB, polished and implanted emitters compared with the  $\text{POCl}_3$  emitter is the main reason why the  $J_{0e}$  (see Fig. 3) values are lower and the  $V_{oc}$  values are higher (see Table 2).

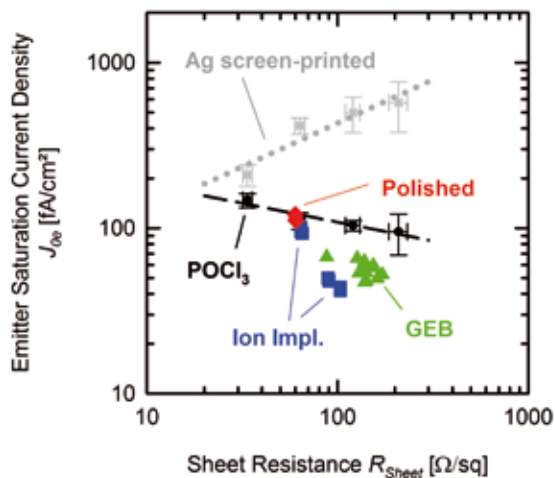


Figure 3. Emitter saturation current density of homogeneously  $\text{POCl}_3$ -diffused emitters with Ag screen-printed contacts (grey), as well as a  $\text{SiN}_x$  surface passivation (black) [21]. The emitter saturation current densities of the GEB (green) and ion-implanted (blue) emitters are significantly lower than for  $\text{POCl}_3$ -diffused emitters with the same sheet resistance.

earlier for the reference PERC process.

This very lean PERC process flow requires just 10 process steps. The schematic cross section of the resulting PERC solar cell is basically identical to the reference PERC cell in Fig. 1 (left). However, the rear surface of the polished PERC cell is slightly rougher, and the doping profile of the emitter is different from that of the reference PERC cell.

**D) GEB PERC: PERC solar cells with selective emitter formed by gas phase etch-back**

See Hannebauer et al. [20] for an in-depth description of the novel selective emitter process for GEB PERC cells. The wafers are double-sided textured and double-sided POCl<sub>3</sub> diffused, with an emitter sheet resistance of 45Ω/sq. Using an inkjet printer, an etch barrier (barrier material provided by Merck) is printed on the front side of the wafer in areas where the front Ag fingers will later also be screen printed. The printed etch barrier width is around 600µm, which is subject to further reduction and optimization.

The rear side is then polished using the RENA InPilot tool, and the emitter is thereby simultaneously etched back on the front side in between the etch barrier fingers by the reactive gas phase of the polish bath. In contrast with the previously described polished PERC process, the polish recipe is adjusted in order to obtain a much more reactive gas phase which removes about 30 to 40nm of the phosphorus emitter on the front side while wet chemically polishing and removing about 8µm of silicon on the rear side. The cleaning after the polish removes the etch barrier.

The final emitter sheet resistances are about 90Ω/sq. in between the etch barrier fingers (later SiN<sub>x</sub> passivated), and about 45Ω/sq. below the etch barrier (later Ag screen printed). The passivation of the rear and front surfaces, the LCO and the screen printing of the front and rear contacts are carried out as described earlier for the reference PERC process. Compared

with the polished PERC cells, the GEB PERC process flow requires just one additional process step (etch barrier deposition) to form a selective emitter instead of a homogeneously doped emitter. Fig. 1 (right) shows a schematic drawing of the GEB PERC solar cell with selective emitter.

**Emitter doping profiles and saturation currents**

The doping profiles are obtained by electrochemical capacitance-voltage (ECV) measurements of planar test wafers which have been processed in a very similar way to that of the corresponding PERC solar cells. Fig. 2(a) shows the resulting doping profiles; the 70Ω/sq. POCl<sub>3</sub> emitter of the reference PERC cell is shown in black and serves as a reference. The doping profile of the 90Ω/sq. GEB emitter is almost identical to that of the polished PERC cell, since in both cases a 45Ω/sq. POCl<sub>3</sub> diffusion is applied. However, around 40nm of the front surface of the emitter has been removed by the GEB; accordingly, the ECV profile of the GEB emitter is shifted by 40nm in Figs. 2(a) and (b). The doping profile of the 65Ω/sq. ion-implanted emitter after annealing has a depth of around 0.55µm, which is comparable to that for the GEB and polished PERC emitters.

Fig. 2(b) shows a close-up of the first 0.1µm in Fig. 2(a) so that the significantly different phosphorus concentrations at the front surface can be observed. As can be seen, the GEB 90Ω/sq. emitter is etched back by approximately 40nm, resulting in the lowest phosphorus surface concentrations of 5×10<sup>19</sup>cm<sup>-3</sup>. The doping profile of the polished PERC emitter shows a front phosphorus concentration of around 1.5×10<sup>20</sup>cm<sup>-3</sup>, despite the strong 45Ω/sq. POCl<sub>3</sub> diffusion. This is achieved by the aggressive wet cleaning after the rear polishing, which partly etches the emitter front surface. The ion-implanted emitter indicates a low

phosphorus concentration of around 2×10<sup>20</sup>cm<sup>-3</sup> of the front as well, which is achieved by a suitable combination of implant and annealing parameters. In this case, the diffusion mechanism follows a ‘limited source behaviour’ according to Fick’s laws of diffusion, which allows a reduction in the surface concentration of phosphorus, as opposed to the typically ‘unlimited source behaviour’ of POCl<sub>3</sub> diffusion, which maintains the concentration at the surface.

To assess the electrical performance of the different emitters, the emitter saturation current density *J*<sub>0e</sub> is measured by quasi-steady-state photoconductance (QSSPC) of suitable test structures using float zone wafers with resistivities of about 200Ωcm. The GEB, polished and ion-implanted emitters are processed in the same way as the corresponding PERC cells, including a textured surface passivated by SiN<sub>x</sub>.

“The superior performance of the ion-implanted and GEB emitters is due to the significantly lower front-surface phosphorus concentration.”

Measurements taken after firing are shown in Fig. 3. The black data points represent the reference POCl<sub>3</sub> emitter for different sheet resistances and are taken from Hannebauer et al. [21]. The grey data points, labelled ‘Ag screen-printed’, refer to *J*<sub>0e</sub> measurements by dynamic infrared lifetime mapping (DILM) of Ag screen-printed contacts on POCl<sub>3</sub>-diffused emitters with different sheet resistances, as published in Hannebauer et al. [21]. For sheet resistances of 90 to 130Ω/sq. in particular, the ion-implanted and GEB emitters yield significantly lower *J*<sub>0e</sub>.

PERC type	Emitter technology	Emitter doping	η [%]	V <sub>oc</sub> [mV]	J <sub>sc</sub> [mA/cm <sup>2</sup> ]	FF [%]
Ref. PERC	POCl <sub>3</sub>	H, 70Ω/sq.	20.0	649	38.1	80.9
I <sup>2</sup> -PERC	Ion implantation	H, 65Ω/sq.	20.0	659	38.7	78.3
Polished PERC	POCl <sub>3</sub>	H, 65Ω/sq.	20.2	655	38.0	81.0
GEB PERC	GEB	SE, 90/45Ω/sq.	20.3*	660	38.3	80.3

\*Independently confirmed by ISE CalLab

**Table 2. Solar cell parameters of the best PERC solar cell of each process flow, measured under standard testing conditions (H = homogeneously doped; SE = selective emitter).**

values of 40 to 60fA/cm<sup>2</sup>, compared with 90fA/cm<sup>2</sup> for the POCl<sub>3</sub>-diffused emitter. The superior performance of the ion-implanted and GEB emitters is due to the significantly lower front-surface phosphorus concentration, as shown in Fig. 2(b), resulting in fewer inactive phosphorus atoms which could act as recombination centres. For the polished PERC cells, however, the  $J_{0e}$  values of around 110fA/cm<sup>2</sup> are comparable to the current densities for POCl<sub>3</sub>-diffused emitters of the same sheet resistance.

## PERC solar cells

Table 2 shows the  $I$ - $V$  parameters of the best performing PERC cells of the four PERC cell process flows described earlier. The reference PERC cell demonstrates a conversion efficiency  $\eta$  of 20.0%, whereas the polished and GEB PERC cells yield conversion efficiencies of 20.2% and 20.3% respectively. The benefit of the selective emitter of the GEB PERC cell can be seen in the high open-circuit voltage  $V_{oc}$  of 660mV and good short-circuit density  $J_{sc}$  of 38.3mA/cm<sup>2</sup>. The I<sup>2</sup>-PERC cell achieves 20.0% conversion efficiency and high  $V_{oc}$  and  $J_{sc}$  values; the fill factor  $FF$ , however, is significantly lower than for the other PERC cells. It has to be considered, though, that the I<sup>2</sup>-PERC cell has been produced using an older process, with respect to the rear-surface passivation and front-side metallization, than in the case of the other three PERC cells, which have been created using the latest process at ISFH. If the latest process is applied to the I<sup>2</sup>-PERC cells, the conversion efficiency is expected to be around 20.2%.

Another option for further increasing the conversion efficiency of I<sup>2</sup>-PERC cells is to apply a selective emitter by putting a shadow mask in the ion beam, a technique which requires no additional process step [12]. Moreover, it should be mentioned that the GEB PERC cells stem from only the fourth batch ever of cells processed using this novel selective emitter concept. The etch barrier still has improvement potential with respect to the barrier width and the etch resistance. Efficiencies higher by at least 0.2% abs. are therefore expected with an optimized GEB PERC cell process in the future.

“Efficiencies higher by at least 0.2% abs. are expected with an optimized GEB PERC cell process in the future.”

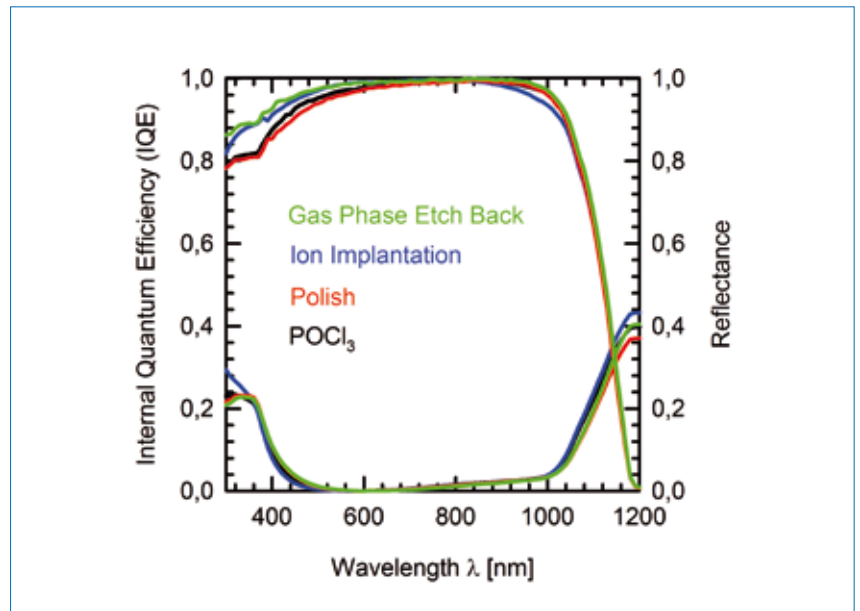


Figure 4. IQE (top) and reflectance (bottom) measurements of the GEB PERC cell, the I<sup>2</sup>-PERC cell, the polished PERC cell and the reference PERC cell (POCl<sub>3</sub>) in Table 2. The improved IQE in the blue-wavelength regime of the GEB and I<sup>2</sup>-PERC cells compared with the reference PERC cell is in accordance with the lower  $J_{0e}$  values shown in Fig. 3. The slightly lower IQE of the I<sup>2</sup>-PERC cell in the infrared-wavelength regime is due to the older rear-passivation process.

To compare the performance of the different phosphorus emitters, the internal quantum efficiency (IQE) and reflectance of the four PERC cells of Table 2 were measured. As can be seen in Fig. 4, the GEB PERC and the I<sup>2</sup>-PERC cells show a significantly improved blue-wavelength IQE compared with the reference PERC cell. Accordingly, the lower  $J_{0e}$  values of the ion-implanted emitter and the GEB emitter compared with the POCl<sub>3</sub> emitter in Fig. 3 translate into a higher blue-wavelength IQE, and hence into higher  $V_{oc}$  and  $J_{sc}$  values, as shown in Table 2.

Fig. 4 also indicates that the IQE of the I<sup>2</sup>-PERC cell is slightly lower in the infrared regime around 1000nm wavelength; this is caused by the older rear-passivation process and is not related to the emitter formation. The IQE of the polished PERC cell is almost identical to that of the reference PERC cell, despite the different types of POCl<sub>3</sub> diffusion used in the process flows. The wet chemical etch-back of the emitter of the polished PERC cell therefore compensates for the stronger POCl<sub>3</sub> diffusion. Furthermore, in the red-wavelength regime the IQEs of the GEB and polished PERC cells are comparable to the IQE of the reference PERC cell, which proves that the rear polish is sufficient to allow an excellent rear-surface passivation.

## Conclusions

Emitter technologies of three industrially applicable PERC cell concepts have been evaluated, including ion-implanted emitter, chemically polished rear surface, and selective emitter by GEB. The results were compared with a high-efficiency reference PERC cell. The three industrial PERC concepts employ lean industrially applicable process sequences which reduce the phosphorus concentration at the wafer surface.

“When applied to PERC cells, the ion-implanted and GEB emitters achieve conversion efficiencies of up to 20.3%.”

The ion-implanted and GEB emitters consequently obtain significantly reduced emitter saturation current densities of 40 to 60fA/cm<sup>2</sup> for emitter sheet resistances of 90 to 130Ω/sq. When applied to PERC cells, the ion-implanted and GEB emitters demonstrate up to 10mV higher open-circuit voltages than the POCl<sub>3</sub>-diffused reference PERC cell and achieve conversion efficiencies of up to 20.3%. The potential for further increases in efficiency has been discussed.

## Acknowledgements

We thank our colleagues at ISFH for their support in the processing of the solar cells. This work was funded in part by the German Federal Ministry for the Environment, Nature Conservation and Nuclear Safety within the HighScreen R&D project and by our industry partners Singulus Technologies, RENA, Heraeus, Solar World and Applied Materials.

## References

- [1] Blakers, A.W. et al. 1989, "22.8% efficient silicon solar cell", *Appl. Phys. Lett.*, Vol. 55, p. 1363.
- [2] Klöter, B. et al. 2013, "Current status of high-efficiency Q.ANTUM technology at Hanwha Q.Cells", *Proc. 39th IEEE PVSC*, Tampa, Florida, USA [in press].
- [3] Zhao, J. 2013, "A 20% efficient PERC type cell and prospects for the future of high efficiency cell technologies", *Proc. 39th IEEE PVSC*, Tampa, Florida, USA [in press].
- [4] Xia, Z. et al. 2013, "Rear side dielectrics choices in PERC solar cells", *Proc. 39th IEEE PVSC*, Tampa, Florida, USA [in press].
- [5] Weber, T. et al. 2013, "High volume pilot production of high efficiency PERC solar cells – analysis based on device simulation", *Proc. 4th SiliconPV Conf.*, Hamelin, Germany [in press].
- [6] Lachowicz, A. et al. 2012, "NO<sub>x</sub>-free solution for emitter etch-back", *Proc. 27th EU PVSEC*, Frankfurt, Germany, p. 1846.
- [7] Dullweber, T. et al. 2012, "Towards 20% efficient large-area screen-printed rear-passivated silicon solar cells", *Prog. Photovolt.: Res. Appl.*, Vol. 20, pp. 630–638.
- [8] Lai, J.H. et al. 2011, "Large area 19.6% efficient rear passivated silicon solar cells with local Al BSF and screen printed contacts", *Proc. 37th IEEE PVSC*, Seattle, Washington, USA, pp. 1929–1932.
- [9] Haverkamp, H. et al. 2008, "Minimizing the electrical losses on the front side: Development of a selective emitter process from a single diffusion", *Proc. 33rd IEEE PVSC*, San Diego, California, USA, pp. 430–433.
- [10] Antoniadis, H. et al. 2010, "All screen printed mass produced silicon ink selective emitter solar cells", *Proc. 35th IEEE PVSC*, Honolulu, Hawaii, USA, pp. 1193–1196.
- [11] Köhler, J.R. et al. 2009, "Laser doped selective emitters yield 0.5% efficiency gain", *Proc. 24th*

*EU PVSEC*, Hamburg, Germany, pp. 1847–1850.

- [12] Jäger, U. et al. 2009, "Selective emitter by laser doping from phosphorus silicate glass", *Proc. 24th EU PVSEC*, Hamburg, Germany, pp. 1740–1743.
- [13] Dubé, C.E. et al. 2011, "High efficiency selective emitter cells using patterned ion implantation", *Energy Procedia*, Vol. 8, pp. 706–711.
- [14] Hahn, G. 2010, "Status of selective emitter technology", *Proc. 25th EU PVSEC*, Valencia, Spain, pp. 1091–1096.
- [15] Gatz, S. et al. 2012, "Analysis and optimization of the bulk and rear recombination of screen-printed PERC solar cells", *Energy Procedia*, Vol. 27, pp. 95–102.
- [16] Müller, J. et al. 2011, "Contact formation and recombination at screen-printed local aluminum-alloyed silicon solar cell base contacts", *IEEE Trans. Electron. Dev.*, Vol. 58, No. 10, pp. 3239–3245.
- [17] Hannebauer, H. et al. 2013, "Record low Ag paste consumption of 67.7 mg with dual print", 4th Metalliz. Worksh., Constance, Germany [in press].
- [18] Dullweber, T. et al. 2013, "Ion-implanted PERC solar cells with Al<sub>2</sub>O<sub>3</sub>/SiN<sub>x</sub> rear passivation", *Proc. 4th SiliconPV*, Hamelin, Germany [in press].
- [19] Kranz, C. et al. 2013, "Wet chemical polishing for industrial type PERC solar cells", *Proc. 4th SiliconPV*, Hamelin, Germany [in press].
- [20] Hannebauer, H. et al. 2013, "Gas phase etch back: A new selective emitter technology for high-efficiency PERC solar cells", *Proc. 28th EU PVSEC*, Paris, France [forthcoming].
- [21] Hannebauer, H. et al. 2012, "Analysis of the emitter saturation current density of industrial type silver screen-printed front contacts", *Proc. 27th EU PVSEC*, Frankfurt, Germany, p. 1360.

## About the Authors



**Thorsten Dullweber** received his Ph.D. from the University of Stuttgart, Germany, in 2002. From 2001 to 2009 he worked as a project leader at Siemens, Infineon and Qimonda. Since 2009 he has led the R&D solar cell production processes group at ISFH, focusing on process and efficiency improvements of industrial-type screen-printed silicon solar cells.



**Helge Hannebauer** studied technical physics at the Leibniz University of Hanover from 2005 to 2009. For his diploma thesis at ISFH he studied the optimization of screen-printed solar cells. He started his Ph.D. degree in 2010, also at ISFH, with a focus on advanced screen printing and selective emitters.



**Christopher Kranz** received his diploma degree in physics from the University of Münster (WWU) in 2011, after which he began a Ph.D. programme at ISFH in the R&D group for solar cell production processes. He currently carries out research on screen-printed solar cells with passivated emitter and rear side.



**Rene Hesse** studied engineering at the University of Applied Sciences in Brandenburg/Havel. Since receiving his diploma degree in 2007, he has worked as an R&D engineer at ISFH, with a focus on screen printing.



**Sabrina Wyczanowski** joined ISFH in 2008 as a technical assistant. She is responsible for the RENA InPilot tool at ISFH, including the development of improved chemical polishing processes. She is also in charge of processing PERC solar cells within different R&D projects at ISFH.



**Vikram Bhosle** received his Ph.D. in materials science and engineering in 2007 from North Carolina State University, USA. His thesis work was related to novel transparent conducting oxide for optoelectronic and photovoltaic devices. He has been with Varian Semiconductor Equipment/Applied Materials since 2011, working on the development of ion implantation and processing for high-efficiency solar cells.



**Chris Dubé** has B.S. and Ph.D. degrees in chemistry and an M.S. in electrical engineering. He started his career in photovoltaics at Mobil Solar Energy Corporation (1982–1992), followed by Evergreen Solar (2004–

2009). Since 2009 he has been with Varian Semiconductor Equipment/Applied Materials, developing and promoting ion implantation for solar cell processing.

**Katrin Weise** studied electrical engineering at the University of Paderborn from 2003 to 2008. She then worked in the PV department at Stiebel Eltron on the industrialization of the RISE EWT solar cell concept that was developed at ISFH. In 2011 she joined the R&D department of RENA GmbH as a process engineer for wet chemical smoothing processes.



**Dr. Oliver Doll** heads the R&D labs of Structuring Solutions within the chemicals business sector of Merck KGaA, Germany. He holds a Ph.D. in the field of inorganic and analytical chemistry.



**Dr. Ingo Koehler** is head of R&D and technical marketing of Structuring Solutions at Merck KGaA, Germany. Since 2007 he has contributed to numerous publications on c-Si PV cell performance. He holds a Ph.D. in the field of semiconductor and solid-state physics and is a member of the scientific advisory board of Fraunhofer ISE PV-TEC, Germany.



**Prof. Rolf Brendel** is the scientific director of ISFH. He received his Ph.D. in materials science from the University of Erlangen, for which he researched infrared spectroscopy. In 2004 he joined the Institute of Solid State Physics of the Leibniz University of Hanover as a full professor. His main research focuses on the physics and technology of crystalline silicon solar cells.



**Franck Delahaye** studied process technology. In 1999 he started PV activities at RENA. He worked on various PV technologies and invented wet processing applications like single side etching. At present he is product manager in the solar division of RENA.

#### Enquiries

Thorsten Dullweber  
Institute for  
Solar Energy Research Hamelin  
(ISFH)

Am Ohrberg 1  
31860 Emmerthal  
Germany

Tel: +49-5151-999-638  
Fax: +49-5151-999-400  
Email: t.dullweber@isfh.de

**rofin**  
LASER MICRO



## Systems for PV manufacturing

- MWT drilling
- Laser doping
- Passivation layer ablation
- Up to 3600 UPH

Visit us at  
EUPVSEC Paris  
01. - 03.10.13  
Hall 2 Booth E15



#### ROFIN-BAASEL Lasertech

Petersbrunner Straße 1b  
82319 Starnberg/Germany  
Tel: +49(0) 8151-776-0  
E-Mail: sales@baasel.de

[www.rofin.com/solar](http://www.rofin.com/solar)

FOCUS ON FINE SOLUTIONS